PAPER

Electron capture to the continuum manifestation in fully differential cross sections for ion impact single ionization

IOP Publishing Journal of Physics B: Atomic, Molecular and Optical Physics
J. Phys. B: At. Mol. Opt. Phys. **51** (2018) 085204 (6pp) https://doi.org/10.1088/1361-6455/aab5dc

Electron capture to the continuum manifestation in fully differential cross sections for ion impact single ionization

M F Ciappina[1], O A Fojón[2] and R D Rivarola[2]

[1] Institute of Physics of the ASCR, ELI-Beamlines project, Na Slovance 2, 182 21 Prague, Czechia
[2] Laboratorio de Colisiones Atómicas, Instituto de Física Rosario, CONICET y Universidad Nacional de Rosario, Bv. 27 de Febrero 210 bis, 2000 Rosario, Argentina

E-mail: marcelo.ciappina@eli-beams.eu

Received 6 December 2017, revised 1 March 2018
Accepted for publication 12 March 2018
Published 4 April 2018

Abstract

We present theoretical calculations of single ionization of He atoms by protons and multiply charged ions. The kinematical conditions are deliberately chosen in such a way that the ejected electron velocity matches the projectile impact velocity. The computed fully differential cross sections (FDCS) in the scattering plane using the continuum-distorted wave-eikonal initial state show a distinct peaked structure for a polar electron emission angle $\theta_k = 0°$. This element is absent when a first order theory is employed. Consequently, we can argue that this peak is a clear manifestation of a three-body effect, not observed before in FDCS. We discuss a possible interpretation of this new feature.

Keywords: ion collisions, two-center effects, distorted wave theories

1. Introduction

The interaction of atoms and molecules with charged particles, such as electrons and heavy ions, and photons is of instrumental interest in the subsequent study in diverse areas of research, e.g. plasma and biological physics (see e.g. [1] and [2] and references therein). Furthermore, the understanding of particle-atom interactions is also important from a fundamental point of view, considering typically we deal with the dynamics of what is known as 'few-body Coulomb problem'. In fact, the processes occurring in collisions of various particles with atoms are particularly suitable to study the complex and highly correlated reaction dynamics in such systems.

Thanks to the development of both the cold target recoil ion momentum spectroscopy [3] and reaction microscope [4] techniques, a complete new branch of collision experiments has emerged. This resulted in a considerable advance in the understanding of the few-body dynamics. With these techniques it is possible to simultaneously measure and fully momentum-analyze all the particles, both the light and heavy ones, which participate in the process (for a review see [5]). As a consequence, from these 'kinematically complete experiments' it is possible to extract fully differential cross sections (FDCS) for a variety of processes and for a large fraction of the total phase space. Initially, experimental efforts focused on studying the few-body dynamics in collisions of charged particles with atomic targets, especially helium (see e.g. [6–18] and for a comprehensive review see [19]).

The workhorse in the theoretical description of single ionization of single and multielectronic atoms by the impact of heavy ions is the continuum-distorted wave-eikonal initial state (CDW-EIS) approach of Crothers and McCann [20]. This approach can be easily extended to the treatment of collisions of heavy particles with mutielectronic targets [21, 22] by reducing the many electron problem to a three-body system consisting of the projectile, the active electron (the one ionized) and the target nucleus together with the frozen core of the passive electrons (the ones not ionized). In addition, the interaction between the heavy ions, the so-called NN interaction, can be easily incorporated in a semiclassical way [23–25]. This theory is able to reproduce FDCS reasonably well for single ionization of helium by highly charged ions in a broad range of projectile velocities (see e.g. [26–31]).

Other approaches were also employed to obtain FDCS ranging from the simple First Born Approximation (FBA), supposedly valid at high enough impact energies where the contributions of higher orders may be disregarded, to more elaborated ones verifying the boundary conditions imposed by the Coulomb interactions present in the final channel of the reaction. Among them, we can cite the three-Coulomb wave-Hartree–Fock (3CW-HF) [32], the three-distorted wave (3DW) [16, 33] and the CCW-PT [34] models.

The 3CW-HF model employs an asymptotically exact three-body-final-state wavefunction that includes all active two-particle interactions to infinite order by means of perturbation theory. A Hartree–Fock wavefunction is used to represent the initial state of the active electron whereas its final state is described through a numerical continuum eigenfunction. In turn, the final-state distorted wave in the 3DW approach is an approximation to the final-state wavefunction satisfying incoming boundary conditions. In the CCW-PT model, the final state is represented by a continuum correlated wavefunction that takes into account the interaction between the projectile and the residual target. The correlated wavefunctions are nonseparable solutions of the wave equation combining the dynamics of the electron motion relative to the target and projectile, satisfying the Redmond's asymptotic conditions corresponding to long range interactions. In this way, this continuum wavefunction includes in a partial way the correlation of the electron-projectile and electron-target relative motion as coupling terms of the wave equation.

In addition, semiclassical calculations were implemented based on three-body classical trajectory Monte Carlo techniques [35], performing a full three-body treatment of the reaction where all interactions are included all the way through the collision. A central model potential based on Hartree–Fock calculations is used to represent the interaction of the target nucleus with both the active electron and the projectile.

2. Theory

We will compute FDCS for single ionization of He by ion impact as a function of the ionized electron momentum $\mathbf{k} = (k, \theta_k, \phi_k)$, being k the magnitude of the vector and θ_k and ϕ_k the corresponding polar and azimuthal angles, respectively, and of the transverse component $\mathbf{q}_\perp$ of the projectile momentum transfer $\mathbf{q} = \mathbf{K}_i - \mathbf{K}_f$, where $\mathbf{K}_i$ ($\mathbf{K}_f$) is the initial (final) momentum of the incoming particle. In our context $\mathbf{q}_\perp \cdot \hat{\mathbf{v}} = 0$, where $\hat{\mathbf{v}}$ is a unit vector that defines the direction of the velocity vector $\mathbf{v}$ of the projectile, parallel to the z-axis of the reference frame with its origin at the center of mass of the target. The FDCS is related to the prior-form of the transition amplitude $T_{fi}^{(-)}(\mathbf{q}_\perp)$ by energy conservation, through the expression

$$\sigma^{(5)}(\mathbf{k}, \mathbf{q}) = \frac{\mathrm{d}^{(5)}\sigma}{\mathrm{d}\mathbf{k}\mathrm{d}\mathbf{q}_\perp} = \frac{(2\pi)^4}{v} |T_{fi}^{(-)}(\mathbf{q}_\perp)|^2 \delta(E_f - E_i), \quad (1)$$

with E_i (E_f) is the initial (final) energy of the complete system. For details, see e.g. [36]. It is important to note that when differential cross sections depend on the transverse component of the momentum transfer $\mathbf{q}_\perp$ or on the projectile scattering angle, for example, the NN interaction must be included in the formulation since it may play a relevant role in the corresponding calculations, depending on the energies of the emitted electron and momentum transfer value [39]. On the other hand, when differential cross sections depending only on the electron energy and/or angular coordinates are considered, this interaction is not included since their influence in the transition amplitude are reduced to a complex phase factor that gives no contribution to the cross sections (for details, see e.g. [23, 36]). Invoking the eikonal approximation, the NN interaction can be included in the transition amplitude $\mathcal{A}_{if}(\boldsymbol{\rho})$, multiplying it by a phase factor, which for a pure Coulomb internuclear interaction yields:

$$\mathcal{A}_{if}(\boldsymbol{\rho}) = \mathrm{i}(\rho v)^{2\mathrm{i}\nu} \mathcal{A}'_{if}(\boldsymbol{\rho}) \quad (2)$$

with $\nu = Z_P Z_T / v$, Z_P, Z_T and v being the projectile and residual-target ion charges and the projectile velocity, respectively, and where $\boldsymbol{\rho}$ defines the so-called impact parameter ($\boldsymbol{\rho} \cdot \mathbf{v} = 0$). $\mathcal{A}_{\mathrm{if}}(\boldsymbol{\rho})$ ($\mathcal{A}'_{if}(\boldsymbol{\rho})$) is the transition amplitude with (without) the NN interaction. Using a two-dimensional Fourier transform it is possible to find a relation between $\mathcal{A}_{if}(\boldsymbol{\rho})$ and $T_{fi}^{(-)}(\mathbf{q}_\perp)$, i.e. the transition matrices as a function of the impact parameter $\boldsymbol{\rho}$ or the transverse component of the momentum transfer $\mathbf{q}_\perp$. Consequently, the transition matrices with and without the NN interaction can be written as:

$$T'^{(-)}_{fi}(\mathbf{q}_\perp) = \frac{1}{2\pi} \int \mathrm{d}\boldsymbol{\rho}\, \mathrm{e}^{\mathrm{i}\mathbf{q}_\perp \cdot \boldsymbol{\rho}} \mathcal{A}'_{if}(\boldsymbol{\rho}) \quad (3)$$

$$T^{(-)}_{fi}(\mathbf{q}_\perp) = \frac{\mathrm{i}\nu^{2\mathrm{i}\nu}}{2\pi} \int \mathrm{d}\boldsymbol{\rho}\, \rho^{2\mathrm{i}\nu} \mathrm{e}^{\mathrm{i}\mathbf{q}_\perp \cdot \boldsymbol{\rho}} \mathcal{A}'_{if}(\boldsymbol{\rho}), \quad (4)$$

respectively. Applying the inverse Fourier transform in equation (3) and replacing it in equation (4), results

$$T^{(-)}_{fi}(\mathbf{q}_\perp) = \frac{\mathrm{i}\nu^{2\mathrm{i}\nu}}{(2\pi)^2} \int \mathrm{d}\mathbf{q}'_\perp T'^{(-)}_{fi}(\mathbf{q}'_\perp) \int \mathrm{d}\boldsymbol{\rho}\, \rho^{2\mathrm{i}\nu} \mathrm{e}^{\mathrm{i}(\mathbf{q}_\perp - \mathbf{q}'_\perp)\cdot\boldsymbol{\rho}}. \quad (5)$$

The two-dimensional integral over the impact parameter can be done analytically to finally obtain:

$$T^{(-)}_{\mathrm{fi}}(\mathbf{q}_\perp) = \nu \frac{\mathrm{i}\nu^{2\mathrm{i}\nu}(2\pi)^{-\mathrm{i}\nu}}{2^4\pi^3} \int \mathrm{d}\mathbf{q}'_\perp T'^{(-)}_{\mathrm{fi}}(\mathbf{q}'_\perp) |\mathbf{q}_\perp - \mathbf{q}'_\perp|^{-2(1+\mathrm{i}\nu)}. \quad (6)$$

The last integral in equation (6) is evaluated numerically using quadratures. As it is well known, the eikonal approximation is valid as long as (i) the projectile suffers very small deflections in the collision (the so-called straight line approximation) and (ii) the velocity of the recoil ion remains small compared to that of the emitted electron. At the high impact energies used in the present work condition (i) is always fulfilled. Additionally, because of the large recoil-ion to electron mass ratio, condition (ii) is always satisfied.

We use non-orthogonal Jacobi coordinates ($\mathbf{r}_P$, $\mathbf{r}_T$) to describe the ionization process. These coordinates represent the position of the active electron with respect to the incoming

projectile ($\mathbf{r}_P$) and the target ion ($\mathbf{r}_T$), respectively. $\mathbf{R}_T$ is also needed, representing the position of the heavy projectile with respect to the center of mass (CM) of the subsystem *e*-*T*. If we neglect terms of orders $1/M_T$ and $1/M_P$, where M_T and M_P are the masses of the target ion nucleus and incident heavy ion, respectively, we can write $\mathbf{R}_T = \mathbf{r}_T - \mathbf{r}_P$. Within the prior CDW-EIS model, the transition amplitude can then be computed as:

$$T_{fi}^{(-)} = \langle \chi_f^{-\mathrm{CDW}} | W_i | \chi_i^{+\mathrm{EIS}} \rangle, \tag{7}$$

where the initial (final) state distorted wave $\chi_i^{+\mathrm{EIS}}(\chi_f^{-\mathrm{CDW}})$ is an approximation to the initial (final) state which satisfies the outgoing-wave (+) (incoming-wave (−)) asymptotic conditions. For the initial state the asymptotic form of the Coulomb distortion, the so-called eikonal phase, is used in the electron-projectile interaction together with a semi-analytical Rothan-Hartree–Fock description for the initial bound-state wavefunction [37]:

$$\chi_i^{+\mathrm{EIS}} = (2\pi)^{-3/2} \exp(\mathrm{i}\mathbf{K}_i \cdot \mathbf{R}_T) \psi_{\mathrm{RHF}}(\mathbf{r}_T) \mathcal{E}_v^+(\mathbf{r}_P) \tag{8}$$

where $\mathcal{E}_v^+(\mathbf{r}_P)$ is

$$\mathcal{E}_v^+(\mathbf{r}_P) = \exp\left[-\mathrm{i}\frac{Z_P}{v} \ln(v r_P - \mathbf{v} \cdot \mathbf{r}_P) \right] \tag{9}$$

and $\psi_{\mathrm{HF}}(\mathbf{r}_T)$

$$\psi_{\mathrm{RHF}}(\mathbf{r}_T) = \sum_{i=1}^{5} N_i \mathrm{e}^{-\zeta_i r_T}. \tag{10}$$

The normalization factors N_i and effective charges ζ_i are obtained from [37].

The final-state wavefunction is cast into the form:

$$\chi_f^{-\mathrm{CDW}} = (2\pi)^{-3/2} \exp(\mathrm{i}\mathbf{K}_f \cdot \mathbf{R}_T) \chi_T^-(\mathbf{r}_T) C_P^-(\mathbf{r}_P), \tag{11}$$

where $C_P^-(\mathbf{r}_P)$ represents the Coulomb distortion of the ejected electron wavefunction due to the projectile:

$$C_P^-(\mathbf{r}_P) = N(\nu_P) {}_1F_1(-\mathrm{i}\nu_P, 1, -\mathrm{i}k_P r_P - \mathrm{i}\mathbf{k}_P \cdot \mathbf{r}_P). \tag{12}$$

$\nu_P = \frac{Z_P}{k_P}$ is the Sommerfeld parameter, $\mathbf{k}_P$ is the relative momentum of the *e*-*P* subsystem and $N(\nu)$ the usual Coulomb factor, defined as

$$N(\nu_P) = \Gamma(1 - \mathrm{i}\nu_P) \exp(\pi\nu_P/2). \tag{13}$$

Additionally, the wavefunction of the ejected electron in field of the target-residual-ion $\chi_T^-(\mathbf{r}_T)$ can be written as

$$\chi_T^-(\mathbf{r}_T) = (2\pi)^{-3/2} \exp(\mathrm{i}\mathbf{k}_T \cdot \mathbf{r}_T) N(\nu_T) \times {}_1F_1(-\mathrm{i}\nu_T, 1, -\mathrm{i}k_T r_T - \mathrm{i}\mathbf{k}_T \cdot \mathbf{r}_T). \tag{14}$$

Here, $\nu_T = \frac{Z_T}{k_T}$ and $\mathbf{k}_T$ are is the Sommerfeld parameter and the relative momentum of the *e*-*T* subsystem, respectively. Finally, the perturbation potential W_i in equation (7) is defined by

$$(H_i - E_i)\chi_i^{+\mathrm{EIS}} = W_i \chi_i^{+\mathrm{EIS}}, \tag{15}$$

where H_i is the full electronic initial Hamiltonian, neglecting the total CM motion, and E_i is the total initial energy of the system in the CM frame. Particularly, W_i is composed of two differential operators [38], i.e.

$$W_i = \frac{1}{2}\nabla_{\mathbf{r}_P}^2 - \nabla_{\mathbf{r}_P} \cdot \nabla_{\mathbf{r}_T}. \tag{16}$$

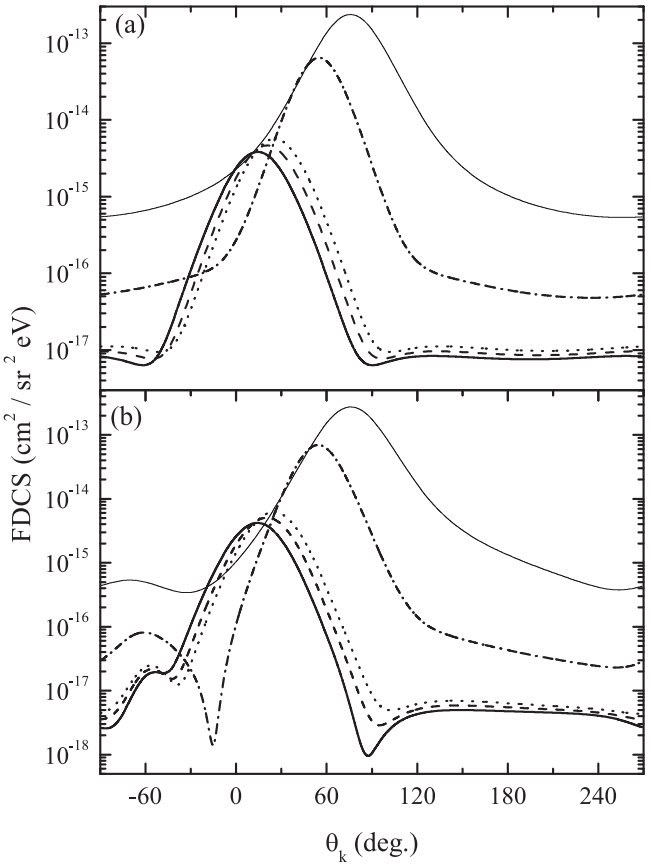

Figure 1. Theoretical (FBA) FDCS for single ionization of He by 500 keV amu^{-1} proton impact. Panel (a) FBA without the NN interaction, panel (b): FBA with NN. The electrons are ejected into the scattering plane as a function of the polar electron emission angle θ_k. The magnitude of the momentum transfer q is fixed at 2.5 a.u. Solid thin curve: $E_k = 50$ eV, dashed–dotted curve: $E_k = 150$ eV, dotted curve: $E_k = 250$ eV, dash curve: $E_k = 260$ eV and thick solid curve: $E_k = 270$ eV.

3. Results and discussion

In the present contribution the CDW-EIS approach has been applied in order to compute FDCS for single ionization of He atoms by impact of protons p^+ and C^{6+} projectiles at 500 keV amu^{-1} ($v = 4.47$ a.u.). In addition, for the case of protons, the FBA is employed as well (for details about the FBA see e.g. [1]).

In figure 1, theoretical single ionization of He by proton p^+ impact FDCS for electrons emitted with different energies, namely 50 eV ($v_e = 1.92$ a.u.) (solid thin line), 150 eV ($v_e = 3.32$ a.u.) (dashed–dotted line), 250 eV ($v_e = 4.28$ a.u.) (dotted line), 260 eV ($v_e = 4.37$ a.u.) (dashed line) and 270 eV ($v_e = 4.45$ a.u.) (solid thick line) into the scattering plane (coplanar geometry), as a function of the polar electron

emission angle θ_k, are shown (note that in atomic units the electron momentum k is equal to its velocity v_e). It should be noted that in the present work, we choose to describe the collision in a plane defined by a pair of orthogonal coordinates (x, z) considering that θ_k varies in the interval (0°, 270°) following the clockwise direction and (0°, −90°) in the counterclockwise one, with 0° coinciding with the positive z-axis.

The magnitude of the momentum transfer was chosen to be $q = 2.5$ a.u. in order to fulfill the energy and momentum conservation laws. In panel (a) calculations neglecting the NN interaction are shown. On the contrary, panel (b) presents FDCS including the NN interaction. In both cases the FBA is used.

The FDCS of figure 1 present the usual binary peaks, whose angular positions, as expected, tend to present their maxima at smaller angles θ_k as the electron emission energy increases. This behavior comes from the fact that the binary peak is expected to appear when $\mathbf{q} = \mathbf{k}$ with $\mathbf{q} = \mathbf{q}_\perp + \left(\frac{E_k - \varepsilon_i}{v}\right)\hat{v}$, where $E_k = k^2/2$ (ε_i) is the final continuum (initial bound) state energy of the electron. Thus, as k increases, for a fixed modulus of $\mathbf{q}$, the longitudinal component of $\mathbf{k}$ also increases whereas the perpendicular one decreases and thus θ_k moves towards smaller angles. For highly charged projectiles, post-collisional effects, due to the projectile attraction of the electrons, reorients their directions and modify the binary collisions as well (a detailed description of this effect can be found in [1], where an extensive review of published contributions is done). However, this effect is less noticeable for the binary encounter peaks. No evidence of the recoil peak is observed under the kinematical conditions here considered.

The same behavior is observed in both panels of figure 2, where we show FDCS computed using the CDW-EIS, under the same kinematical conditions. Additionally, in both panels of figure 2, we clearly observe now the appearance of a peaked structure for $\theta_k = 0°$, totally absent in the first order calculations of figure 1, when the velocity of the ejected electron is close to the one of the projectile. We can argue that it corresponds to the two-center mechanism of electron capture to the continuum (ECC), where the electron ejected from the target is attracted by the projectile field, moving finally with a velocity close to the projectile one (see for example [1, 40, 41]). It is interesting to remark that, as it was shown by Dettmann *et al* [42] (see also [1]), the quantum mechanical reaction associated with the classical two-step Thomas's mechanism [43] gives a negligible contribution to the ECC except at asymptotic high collision velocities.

Finally, in figure 3 we present the same set of calculations of figures 1 and 2, but now the projectile is a highly charged ion (C^{6+}). As expected, the ECC peak is also present for this collision system. Furthermore, both in figures 2 and 3 it is observed that the binary encounter peak overlaps with the ECC one as the final ejection velocity tends to the projectile one. This effect, which is even more noticeable for the C^{6+} impact, may be attributed to the Z_P^2 increasing with the

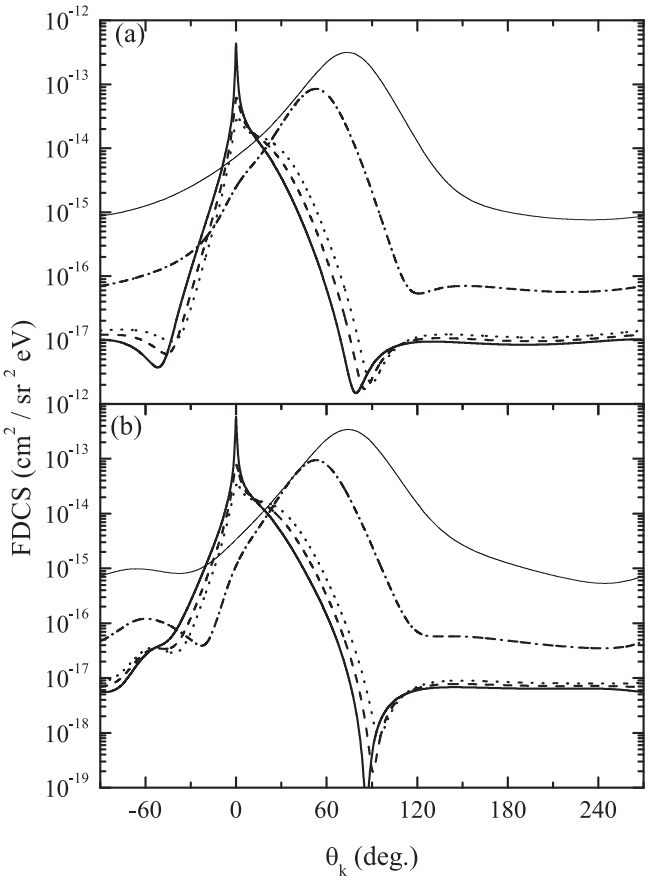

Figure 2. Theoretical (CDW-EIS) FDCS for single ionization of He by 500 keV amu^{-1} proton impact. Panel (a) CDW-EIS without the NN interaction, panel (b): CDW-EIS with NN. The electrons are ejected into the scattering plane as a function of the polar electron emission angle θ_k. The magnitude of the momentum transfer q is fixed at 2.5 a.u. Solid thin curve: $E_k = 50$ eV, dashed–dotted curve: $E_k = 150$ eV, dotted curve: $E_k = 250$ eV, dash curve: $E_k = 260$ eV and thick solid curve: $E_k = 270$ eV.

projectile charge in a binary encounter between the projectile and the active electron.

For proton impact, in both FBA and CDW-EIS descriptions and when the NN interaction is included in calculations, a peak appears at $\theta_k \simeq -60°$. We must mention that some structures were also experimentally found for $\theta_k = \theta_q$ (where θ_q is the direction of $\mathbf{q}$) and electron energy $E_k = 5.4$ eV at smaller collision energies for 75 keV protons interacting with He atoms [44]. However these structures were only reproduced for high enough transverse momentum transfer, using a theoretical model where a Born initial wavefunction and a final continuum one which includes the dynamical correlation of the electron-projectile and electron-residual target relative motion and the interaction between the projectile and the residual target are employed [45]. Qualitative discrepancies with measurements were found for small transverse momentum transfers. A similar situation occurs when the 3DW model is employed [46]. These authors speculated that a possible origin of the experimental existence of these structures could come from a geometrical situation where the residual-target ion stays between the projectile and the active electron, in such way that the interaction of the projectile with the residual target is

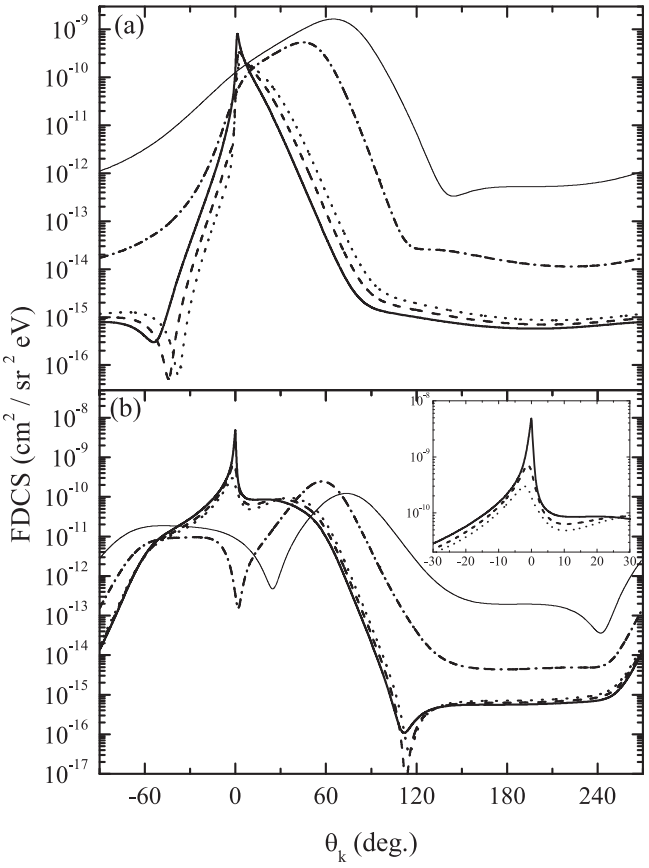

Figure 3. Theoretical (CDW-EIS) FDCS for single ionization of He by 500 keV amu^{-1} C^{6+} impact. Panel (a) CDW-EIS without the NN interaction, panel (b): CDW-EIS with NN. The electrons are ejected into the scattering plane as a function of the polar electron emission angle θ_k. The magnitude of the momentum transfer q is fixed at 2.5 a.u. Solid thin curve: $E_k = 50$ eV, dashed–dotted curve: $E_k = 150$ eV, dotted curve: $E_k = 250$ eV, dash curve: $E_k = 260$ eV and thick solid curve: $E_k = 270$ eV. The inset in panel (b) shows a zoomed region for $\theta_k \in [-30°, 30°]$.

stronger than with the electron. Thus, the transverse momentum transfer is opposite to the one of q_e while the longitudinal component is still in the forward direction. This assumption was inspired from a classical description of an ionization mechanism proposed by Fiol and Olson [47] where a Monte Carlo model was employed to study the ionization of ground and excited state hydrogen by 3.6 MeV u^{-1} C^{6+} and Au^{53+} ions. However, an alternative proposed explanation was that recoil electrons are shifted to the forward direction by the attractive potential created by the projectile. In our case we employ the CDW-EIS model, which is a higher-order theory where successive interactions between the incoming projectile with both the electron and the residual target ion are implicitly taken into account. This is done through the inclusion of distorting factors depending on the projectile-electron potential and the exponential phase containing the interaction between the projectile and the residual target ion. Thus, we could hypothesize that one possible mechanism is the one which corresponds to a first collision of the projectile with the electron, being both ejected in different half-planes and in a second step the projectile is deviated in the same half-plane that the electron due to its interaction with the residual target [44]. In a classical image, if as mentioned before we consider that the electron suffers a first collision with the projectile, emerging both with the same modulus of the velocity, by energy and impulse balance laws the light particle will be ejected at $\theta_k = -60°$. This electron energy corresponds also to the condition of ECC. The fingerprints of this effect remains also when the electron energy varies as it is shown in figures 1 and 2. However, the physical origin of these structures remains still an open question to discern.

For the C^{6+} system, the observed peak appearing for protons at $\theta_k \simeq -60°$ gives now a broad structure for 50 and 150 eV electron emission energies (see figure 3(b)) and a pronounced shoulder on the left side of the ECC peak for electron velocities closer to the projectile one. A similar behavior, associated with the Z_P^2 dependence of the projectile-electron binary encounter, is also observed on the right side of the ECC peak.

4. Conclusions

To sum up, we have carried out computations of FDCS for single ionization of He by 500 keV proton and C^{6+} impact. The kinematical conditions are chosen to allow ejected electron velocities with values close to the projectile impact velocity. The FBA results show the typical features present in the FDCS, even for ejected electron velocities very close to the projectile one. On the contrary, the CDW-EIS computations present a distinct peaked structure for $\theta_k = 0°$ for both protons and C^{6+} projectiles. This peak can be clearly attributed to an ECC mechanism, considering the CDW-EIS represent a theory that includes higher-order two-center mechanisms. This peak could be, in principle, experimentally observed. The kinematical conditions to make it visible, however, can prevent measuring it, considering, on the one hand, the small FDCS values, and, on the other hand, the narrowness of the peak, that would require an angular resolution difficult to reach.

Acknowledgments

This work was supported by the project ELI—Extreme Light Infrastructure—phase 2 (CZ.02.1.01/0.0/0.0/15 008/0000162) and the project Advanced research using high intensity laser produced photons and particles (CZ.02.1.01/0.0/0.0/16 019/0000789) both from the European Regional Development Fund. RDR and OAF acknowledge financial support from PICT 2015-3329 of the Agencia Nacional de Promoción Científica y Tecnológica of Argentina and PIP 0784 from CONICET.

ORCID iDs

M F Ciappina https://orcid.org/0000-0002-1123-6460

References

[1] Stolterfoht N, DuBois R D and Rivarola R D 1997 *Electron Emission in Heavy Ion-Atom Collisions* (Berlin: Springer) (https://doi.org/10.1007/978-3-662-03480-4)
[2] Drake G W F (ed) 2006 *Springer Handbook of Atomic, Molecular, and Optical Physics* (Berlin: Springer)
[3] Ullrich J, Moshammer R, Dörner R, Jagutzki O, Mergel V, Schmidt-Böcking H and Spielberger L 1997 *J. Phys. B: At. Mol. Opt. Phys.* **30** 2917
[4] Ullrich J, Moshammer R, Dorn A, Dörner R, Schmidt L P H and Schmidt-Böcking H 2003 *Rep. Prog. Phys.* **66** 1463
[5] Dörner R, Mergel V, Jagutzski O, Spielberger L, Ullrich J, Moshammer R and Schmidt-Böcking H 2000 *Phys. Rep.* **330** 95
[6] Schulz M, Moshammer R, Fischer D, Kollmus H, Madison D H, Jones S and Ullrich J 2003 *Nature* **422** 48
[7] Maydanyuk N V, Hasan A, Foster M, Tooke B, Nanni E, Madison D H and Schulz M 2005 *Phys. Rev. Lett.* **94** 243201
[8] An L, Khayyat K and Schulz M 2001 *Phys. Rev.* A **63** 030703
[9] Schulz M *et al* 2001 *J. Phys. B: At. Mol. Opt. Phys.* **34** L305
[10] Schulz M, Moshammer R, Perumal A N and Ullrich J 2002 *J. Phys. B: At. Mol. Opt. Phys.* **35** L161
[11] Fischer D, Moshammer R, Schulz M, Voitkiv A and Ullrich J 2003 *J. Phys. B: At. Mol. Opt. Phys.* **36** 3555
[12] Voitkiv A B, Najjari B, Moshammer R, Schulz M and Ullrich J 2004 *J. Phys. B: At. Mol. Opt. Phys.* **37** L365
[13] Schulz M, Moshammer R, Voitkiv A, Najjari B and Ullrich J 2005 *Nucl. Instrum. Methods Phys. Res.* B **235** 296
[14] Schulz M *et al* 2013 *Phys. Rev.* A **88** 022704
[15] Hubele R *et al* 2013 *Phys. Rev. Lett.* **110** 133201
[16] Schulz M, Hasan A, Maydanyuk N V, Foster M, Tooke B and Madison D H 2006 *Phys. Rev.* A **73** 062704
[17] Hasan A, Maydanyuk N V, Fendler B J, Voitkiv A, Najjari B and Schulz M 2004 *J. Phys. B: At. Mol. Opt. Phys.* **37** 1923
[18] Ciappina M F, Tachino C A, Rivarola R D, Sharma S and Schulz M 2015 *J. Phys. B: At. Mol. Opt. Phys.* **48** 115204
[19] Schulz M and Madison D H 2006 *Int. J. Mod. Phys.* A **21** 3649
[20] Crothers D S F and McCann J F 1983 *J. Phys. B: At. Mol. Phys.* **16** 3229
[21] Gulyás L and Fainstein P D 1998 *J. Phys. B: At. Mol. Opt. Phys.* **31** 3297
[22] Fainstein P D, Ponce V H and Rivarola R D 1988 *J. Phys. B: At. Mol. Opt. Phys.* **21** 287
[23] Fainstein P D, Ponce V H and Rivarola R D 1991 *J. Phys. B: At. Mol. Opt. Phys.* **24** 3091
[24] Rodríguez V D and Barrachina R O 1998 *Phys. Rev.* A **57** 215
[25] Sanchez M D, Cravero W R and Garibotti C R 2000 *Phys. Rev.* A **61** 062709
[26] Ciappina M F and Cravero W R 2006 *J. Phys. B: At. Mol. Opt. Phys.* **39** 1091
[27] Ciappina M F and Cravero W R 2006 *J. Phys. B: At. Mol. Opt. Phys.* **39** 2183
[28] Ciappina M F, Cravero W R and Schulz M 2007 *J. Phys. B: At. Mol. Opt. Phys.* **40** 2577
[29] Fainstein P D and Gulyás L 2005 *J. Phys. B: At. Mol. Opt. Phys.* **38** 317
[30] Foster M, Madison D H, Peacher J L and Ullrich J 2004 *J. Phys. B: At. Mol. Opt. Phys.* **37** 3797
[31] Pedlow R T, O'Rourke S F C and Crothers D S F 2005 *Phys. Rev.* A **72** 062719
[32] Madison D, Schulz M, Jones S, Foster M, Moshammer M and Ullrich J 2002 *J. Phys. B: At. Mol. Opt. Phys.* **35** 3297
[33] Maydanyuk N V, Hasan A, Foster M, Tooke B, Nanni F, Madison D H and Schulz M 2005 *Phys. Rev. Lett.* **94** 243201
[34] Niu X, Sun S, Wang F and Jia X 2017 *Phys. Rev.* A **96** 022703
[35] Olson R E and Fiol J 2003 *J. Phys. B: At. Mol. Opt. Phys.* **36** L365
[36] Ciappina M F, Fojón A and Rivarola R D 2014 *J. Phys. B: At. Mol. Opt. Phys.* **47** 042001
[37] Clemente E and Roetti C 1974 *At. Data Nucl. Data Tables* **14** 177
[38] Crothers D S F and Dubé L J 1992 *Adv. At. Mol. Opt. Phys.* **30** 287–337
[39] Ciappina M F and Rivarola R D 2008 *J. Phys. B: At. Mol. Opt. Phys.* **41** 015203
[40] Fiol J and Olson R E 2002 *J. Phys. B: At. Mol. Opt. Phys.* **35** 1759
[41] Fiol J, Rodríguez V D and Barrachina 2001 *J. Phys. B: At. Mol. Opt. Phys.* **34** 933
[42] Dettmann K, Harrison K G and Lucas M W 1974 *J. Phys. B: At. Mol. Phys.* **7** 269
[43] Thomas L H 1927 *Proc. R. Soc.* A **114** 561
[44] Schulz M, Hasan A, Maydanyuk N V, Foster M, Tooke B and Madison D N 2006 *Phys. Rev.* A **73** 062704
[45] Niu X, Sun S, Wang F and Jia X 2017 *Phys. Rev.* A **96** 022703
[46] Maydanyuk N V, Hasan A, Foster M, Tooke B, Nanni F, Madison D H and Schulz M 2005 *Phys. Rev. Lett.* **94** 243201
[47] Fiol J and Olson R E 2002 *J. Phys. B: At. Mol. Opt. Phys.* **35** 1759